



HAL
open science

The contralateral synchronous breast carcinoma: a comparison of histology, localization, and magnetic resonance imaging characteristics with the primary index cancer

Diane M. Renz, Joachim Böttcher, Pascal A. T. Baltzer, Matthias Dietzel, Tibor Vag, Mieczyslaw Gajda, Oumar Camara, Ingo B. Runnebaum, Werner A. Kaiser

► **To cite this version:**

Diane M. Renz, Joachim Böttcher, Pascal A. T. Baltzer, Matthias Dietzel, Tibor Vag, et al.. The contralateral synchronous breast carcinoma: a comparison of histology, localization, and magnetic resonance imaging characteristics with the primary index cancer. *Breast Cancer Research and Treatment*, 2010, 120 (2), pp.449-459. 10.1007/s10549-009-0718-1 . hal-00535432

HAL Id: hal-00535432

<https://hal.science/hal-00535432>

Submitted on 11 Nov 2010

HAL is a multi-disciplinary open access archive for the deposit and dissemination of scientific research documents, whether they are published or not. The documents may come from teaching and research institutions in France or abroad, or from public or private research centers.

L'archive ouverte pluridisciplinaire **HAL**, est destinée au dépôt et à la diffusion de documents scientifiques de niveau recherche, publiés ou non, émanant des établissements d'enseignement et de recherche français ou étrangers, des laboratoires publics ou privés.

The contralateral synchronous breast carcinoma: a comparison of histology, localization, and magnetic resonance imaging characteristics with the primary index cancer

Diane M. Renz · Joachim Böttcher · Pascal A. T. Baltzer · Matthias Dietzel · Tibor Vag · Mieczyslaw Gajda · Oumar Camara · Ingo B. Runnebaum · Werner A. Kaiser

Received: 21 December 2009 / Accepted: 23 December 2009 / Published online: 20 January 2010
© Springer Science+Business Media, LLC. 2010

Abstract Women with unilateral breast carcinoma reveal an increased risk of suffering from malignancies in the contralateral breast. There is a controversy about the existence of bilateral phenotypic similarities. The aim of this investigation was to compare histologic findings, magnetic resonance imaging (MRI) parameters, and tumor localizations of synchronous bilateral carcinomas. MRI revealed in 42 of 875 women (4.8%) with primary index carcinomas a contralateral malignancy. Twenty-two of the 42 contralateral carcinomas could only be detected by MRI, not by clinical examination, X-ray mammography, or ultrasonography. In 875 patients, MRI therefore identified 22 (2.5%) otherwise occult contralateral cancers. To evaluate bilateral MRI similarities, multiple dynamic and morphologic parameters were evaluated. Of 42 bilateral cancer pairs, histologic tumor type was identical in 54.8% (correlation analysis, $P < 0.05$). Estrogen receptor status was simultaneously positive or negative in 86.2% ($P < 0.01$), progesterone receptor status in 79.3% ($P < 0.05$), expression of human epidermal growth factor receptor 2 in 76.2% ($P < 0.05$). In 75.8%, initial signal increase, and in 63.6%, postinitial curve types were bilaterally congruent on MRI

($P < 0.05$). Detected masses showed bilaterally similar T2-signal intensity in 81.8% ($P < 0.001$). Similar shape and margin of tumor masses and occurrence of non-mass-like enhancement were also frequently observed in both breasts ($P < 0.05$). The main tumor quadrant was the same in 61.9%, the main localization (retromamillar, central, or dorsal) in 66.7% ($P < 0.01$). Contralateral carcinomas frequently present similar histologic findings, tumor localizations and MRI characteristics reflecting analogies of tumor neoangiogenesis, histopathologic components, and infiltration in the surrounding stroma. Bilateral synchronous carcinomas may represent on each site distinct, but similar biologic entities, due to analogous influences of tumor developments.

Keywords Magnetic resonance imaging · Breast · Primary index carcinoma · Contralateral carcinoma · Bilateral cancer

Introduction

Women with unilateral breast cancer have an increased risk of developing carcinomas in the contralateral breast [1, 2]. This risk is stated to be 2–6 times higher than that for the development of an initial breast malignancy in a woman who has never suffered from breast cancer [3, 4]; the probability is between 0.5 and 1% per year with a cumulative incidence of 15% [2, 3, 5]. In contrast to the risk for recurrence, which decreases after 5–10 disease-free years, the risk for the development of contralateral carcinomas is constantly elevated [5]. In conclusion, the most common second malignant tumor for patients with unilateral breast cancer is a carcinoma in the contralateral breast [2, 3, 5].

D. M. Renz (✉) · J. Böttcher · P. A. T. Baltzer · M. Dietzel · T. Vag · W. A. Kaiser
Institute of Diagnostic and Interventional Radiology,
Friedrich Schiller University Jena, Erlanger Allee 101,
07740 Jena, Germany
e-mail: dianerenz@yahoo.de

M. Gajda
Institute of Pathology, Friedrich Schiller University Jena,
Ziegmühlenweg 1, 07740 Jena, Germany

O. Camara · I. B. Runnebaum
Clinic of Gynecology, Friedrich Schiller University Jena,
Bachstr. 18, 07740 Jena, Germany

The contralateral cancer may be either synchronous, i.e., developing simultaneously, or metachronous, meaning that the tumor manifestation occurs later than the primary one [3, 4, 6]. It remains unclear how many of the metachronous carcinomas were not diagnosed at an earlier stage and therefore not characterized as a synchronously developing cancer manifestation. If the contralateral malignancy is detected delayed after the initial treatment, the patient has to undergo a prolonged and cost-intensive second therapy rather than the single treatment course for both breasts, which would have been administered if the contralateral tumor had been synchronously diagnosed [7, 8]. Thus, an early detection of a possible contralateral breast carcinoma, as best in the stage of a synchronous onset, would provide a major benefit.

Magnetic resonance imaging (MRI) has become a well-established method in the diagnosis and staging of invasive breast carcinomas [9, 10]. MRI achieves the highest sensitivity of all imaging modalities in breast cancer detection reaching 99% [9–16]. MRI has been proven to represent an accurate method in the pre-therapeutic cancer staging for determining the exact tumor size as well as depicting multifocality and multicentricity [12–16]. Recent studies have reported that MRI has also the potential to visualize in X-ray mammography and ultrasonography occult contralateral malignant tumors in women with primary breast cancer; the published detection rates for otherwise missed contralateral carcinomas reached up to 24% [13, 17–21].

There is a controversy if synchronously developing breast carcinomas represent similar biologic characteristics or if they display two completely different sporadic tumor events [1, 6, 22]. Regarding imaging values, similar bilateral tumor phenotypes may lead to analogous MRI appearances and therefore to a more intensely specified characterization of frequently found contralateral lesions in patients with newly diagnosed breast cancer [6, 17, 18, 23]. The purpose of this study was to analyze possible similarities between synchronous bilateral carcinomas. Histologic findings, including hormone receptor status, tumor localization as well as multiple dynamic and morphologic MRI characteristics were evaluated between 42 primary index cancers and their corresponding contralateral carcinomas.

Materials and methods

Patients and reference standards

With a nearly duration of 12 years, the observation period of our investigation was extended. The study design considered the guidelines of the Declaration of Helsinki. The study design was approved by the ethics committee at our university, and all evaluated patients gave their consent for

the scientific use of their clinical and radiological data. All evaluated MRI examinations were acquired at our radiological institute from 22 December 1994 to 16 October 2006 using standardized conditions.

The inclusion criteria were breast MRIs with enhancing lesions and histologic clarification of these lesions. Only women from the clinic of gynecology at our university hospital were included to achieve reliable histologic and clinical data. The indications for MRI were typical indications in a clinical routine setting, such as suspect findings in clinical examination, X-ray mammography, and/or ultrasonography, or cancer research in case of unknown primary. Exclusion criteria were contraindications against MRI examination, such as pacemaker or claustrophobia. In the observation period, 1345 women with histologically proven 917 malignant and 586 benign lesions fulfilled the study criteria (see Fig. 1). The 917 malignant lesions were detected in 875 women: 833 subjects showed unilateral breast cancer, and 42 women presented bilateral malignancies. Thus, contrast-enhanced MRI revealed in 42 of 875 female patients (4.8%) bilateral synchronous malignant lesions.

The ages of the 42 patients with synchronous bilateral carcinomas ranged from 33 to 87 years (mean = 62.9 years, standard deviation (sd) = 11.6 years). Ten of the 42 evaluated women (23.8%) had a positive family history with their mother or at least one sister suffering from invasive breast carcinoma. None of the 42 evaluated subjects underwent breast biopsy in the past 3 months. No woman had received chemotherapy, breast conservation, mastectomy, or radiation therapy prior to MRI. No subject presented severe motion artefacts or hormone effects, which hampered the MRI interpretation.

The breast, in which the most suspected cancer was first detected, either clinically or by X-ray mammography and/or

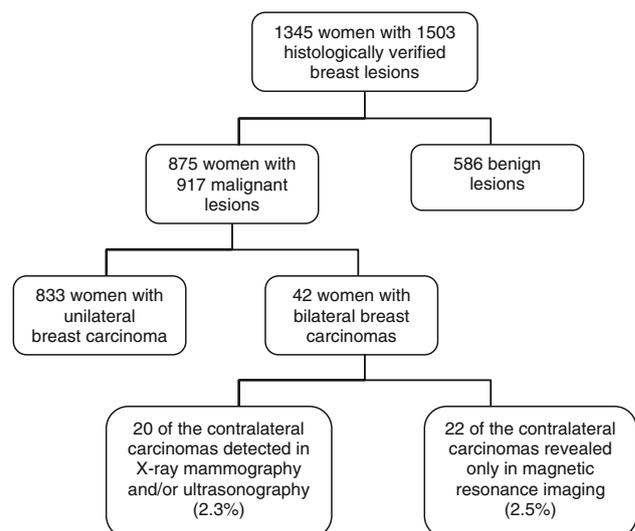


Fig. 1 Flow diagram describes patients' inclusion in the study

ultrasonography, was designated as showing the primary index carcinoma [6, 24, 25]. The simultaneously revealed malignancy in the opposite breast was defined as the contralateral carcinoma [6, 24, 25]. All of the 42 primary index malignancies could be visualized by X-ray mammography and ultrasonography alone or by both imaging modalities. Five of the 42 contralateral carcinomas (11.9%) could only be detected by X-ray mammography and 9.5% (4 of 42) only by ultrasonography. Eleven of 42 contralateral carcinomas (26.2%) were seen in X-ray mammography and ultrasonography. MRI detected 22 of 42 (52.4%) neither by clinical examination nor by X-ray mammography and ultrasonography detectable malignant tumors. In 875 patients, MRI therefore identified 22 (2.5%) otherwise occult contralateral carcinomas (Fig. 1). The contralateral carcinomas, which could be found by other imaging modalities, had a mean diameter of 20 mm (sd = 12 mm); the diameter of the carcinomas, which could only be detected by MRI, was significantly lower: 10 mm (sd = 4 mm; Student's *t*-test; *P* < 0.01).

Magnetic resonance imaging

All MRI examinations were acquired with two technically comparable protocols. The first protocol was used for evaluated examinations until April 2003. Afterwards, the second parameters were utilized in a different MR scanner. All images were obtained by a 1.5-T system using a double breast coil with the patient in a prone position.

Using the first protocol, the images were acquired by a 1.5-T Gyroscan ACSII-scanner (Philips Healthcare, Best, The Netherlands). Multi-slice 2D fast-field-echo (FFE) T1-weighted images were obtained for the dynamic study with the following parameters: repetition time TR 97 ms; echo time TE 5.0 ms; matrix 205 × 256; flip angle 80°; slice thickness 4.0 mm; field of view 350 mm; axial orientation. Axial T2-weighted turbo-spin-echo (TSE) sequences (TR 4000 ms; TE 300 ms; matrix 193 × 256; flip angle 90°; field of view 350 mm) were performed in identical slice positions.

Secondly, the images were acquired by a 1.5-T Siemens system (Symphony; Siemens Medical Solutions, Erlangen, Germany). For this dynamic study, multi-slice 2D FLASH (fast low-angle shot) axial T1-weighted sequences were obtained with the parameters as follows: TR 113 ms; TE 4.6 ms; matrix 384 × 384; flip angle 80°; slice thickness 3.0 mm; field of view 350 mm. Axial T2-weighted TSE sequences (TR 8900 ms; TE 207 ms; matrix 512 × 512; flip angle 90°; field of view 350 mm) were also acquired in identical slice positions.

In both technical protocols, 0.1 mmol/kg body weight gadopentetate dimeglumine (Magnevist; Bayer Schering Pharma, Berlin, Germany) was intravenously injected as a

rapid bolus (flow 3 ml/s) followed by 20-ml saline flush after acquisition of a native T1-weighted sequence. Thirty seconds after bolus injection dynamic imaging was continued with the same technical parameters and under identical tuning conditions at 1-min intervals up to 7 min. Native sequences were subtracted from postcontrast dynamic images.

Image interpretation

All 42 MRI examinations were retrospectively reevaluated in consensus by two radiologists specialized in breast MRI (>500 breast MRIs) analyzing both breasts of a patient. The X-ray mammographies of all 42 patients were also reevaluated in the same manner. For the ultrasonographic results, the written reports of the examinations were used.

For the analysis of the MRI images, dynamic and morphologic parameters were considered using T1- and T2-weighted images. Computer software (Syngo; Siemens Medical Solutions, Erlangen, Germany) was utilized to assess signal intensity time curves in areas of kinetic increase based on contrast enhancement. Three ROIs (regions of interest, 3 × 3 pixels) were placed considering the most enhancing region. If the lesion presented more than one mass, three ROIs were located in each mass. The contrast enhancement was then determined as the mean signal increase of all masses. In absence of masses, the signal characteristic was assessed by placing three ROIs in the most enhancing region of the non-mass-like enhancement. The initial signal increase of the lesion was assessed within the first 90 s after bolus injection considering two categories [26–28]: (1) <100%; (2) >100%. Postinitial contrast enhancement was measured up to 7 min after bolus injection. Three postinitial curve types were defined [26–28]: (1) continuous increase (increase >10%); (2) plateau phenomenon (deviation of the signal curve between +10% and –10%); (3) wash-out sign (decrease >10%). For the analysis of the MRI morphology, the Breast Imaging Reporting and Data System (BI-RADS) atlas [29] and further morphologic characteristics, in detail described in the literature [27, 30, 31], were used.

Histopathology

Histologic diagnoses were performed by an experienced breast pathologist. Carcinomas were categorized by the World Health Organization (WHO) classification of breast cancers. Tumor grading was assessed based on the classification published by Elston and Ellis [32], resulting in well (grade 1), moderately (grade 2), or poorly (grade 3) differentiated carcinomas. Estrogen receptor (ER) and progesterone receptor (PR) status were determined by immunohistochemical methods using antibodies to estrogen

and progesterone receptors. Carcinomas were defined as receptor positive if more than 10% of tumor cells exhibited nuclear staining with the hormone markers used. Expression of human epidermal growth factor receptor 2 (HER 2) was evaluated using antibodies to HER 2; the findings were categorized as positive or negative depending on the presence or absence of membrane staining.

Statistical analysis

At first, the prevalence of all evaluated criteria was separately considered for the carcinomas of the primary index and the opposite breast. Afterwards, the congruence of each parameter was calculated in what percentage the evaluated criterion simultaneously occurred in both breasts. Because some of the evaluated parameters are typical for malignancies, it was determined for dichotomous parameters in what percentage each characteristic simultaneously occurred in both breasts or could not be detected in any of the bilateral carcinomas. The statistical analysis was performed utilizing SPSS version 17.0 for Windows (SPSS; Chicago, IL, USA). Correlation analyses were performed for assessing similarities between characteristics of the corresponding bilateral carcinomas. The Phi correlation coefficient was used for 2×2 contingency tables and the Cramer's *V* coefficient for larger tables. For determining significant differences between the bilateral carcinomas, the Fisher's exact test examined the association between two variables in a 2×2 contingency table. Evaluating variables with more than two categories, the Pearson's chi-square test was performed for analysing differences. The Student's *t*-test was used to examine significant differences between means. A *P* value less than 0.05 (two-sided) was considered to indicate a statistical significance.

Results

Histologic findings and tumor staging

Nearly all of the 42 primary index carcinomas were histologically proven as invasive cancers (Table 1). Two of 42 primary index carcinomas were histopathologically confirmed as ductal carcinomas in situ (DCIS). In comparison, 8 of 42 contralateral tumors were histologically confirmed as in situ carcinomas: 5 DCIS, 2 LCIS, and 1 carcinoma in situ with ductal and lobular features. One patient showed ductal carcinomas in situ at both breasts. Thus, 33 patients presented invasive carcinomas involving both breasts, and 9 women had a non-invasive malignancy at least in one breast. The histologic subtype of the bilateral invasive and non-invasive malignancies (i.e., invasive ductal, lobular, mucinous, or tubular carcinoma as well as DCIS or LCIS)

Table 1 Histologic characteristics of primary index and contralateral carcinomas

	Primary index carcinomas	Contralateral carcinomas
In situ carcinomas		
Ductal carcinoma in situ	4.8% (2/42)	11.9% (5/42)
Lobular carcinoma in situ	0% (0/42)	4.8% (2/42)
Ductal and lobular carcinoma in situ	0% (0/42)	2.4% (1/42)
Invasive carcinomas		
Histologic types		
Invasive ductal	57.5% (23/40)	50.0% (17/34)
Invasive lobular	32.5% (13/40)	35.3% (12/34)
Invasive mucinous	5.0% (2/40)	2.9% (1/34)
Invasive tubular	5.0% (2/40)	11.8% (4/34)
Tumor grading		
G1 (well-differentiated)	10.0% (4/40)	20.6% (7/34)
G2 (moderately differentiated)	55.0% (22/40)	55.9% (19/34)
G3 (poorly differentiated)	35.0% (14/40)	23.5% (8/34)
Receptor status		
Positive estrogen receptor	93.1% (27/29)	79.3% (23/29)
Positive progesterone receptor	86.2% (25/29)	72.4% (21/29)
Positive HER 2 receptor	71.4% (15/21)	66.7% (14/21)

was identical in the two breasts in 54.8% ($n = 23$) of the 42 subjects (Fig. 2); the correlation coefficient Cramer's *V* was 0.436 ($P < 0.05$).

Table 1 shows the tumor grading of the primary index and contralateral invasive carcinomas. The primary index invasive carcinomas presented a higher grade compared with the contralateral invasive malignancies (Pearson's chi-square test; $P < 0.05$). In 29 of 42 bilateral carcinomas, ER and PR status could be evaluated (Table 1). Estrogen receptor status was simultaneously positive or negative in the corresponding bilateral carcinomas in 25 of 29 cases (86.2%; correlation coefficient Phi = 0.533; $P < 0.01$), progesterone receptor status in 79.3% ($n = 23$) of the corresponding synchronous tumors (correlation coefficient Phi = 0.424; $P < 0.05$). In 21 of 42 bilateral carcinomas, the HER 2 status could furthermore be considered; HER 2 was positive or negative in the corresponding carcinomas in 76.2% ($n = 16$ of 21; correlation coefficient Phi = 0.447; $P < 0.05$).

Regarding invasive carcinomas, the average diameter of the 40 invasive primary index tumors was 23 mm (sd = 12 mm; range 7–63 mm). In comparison, the average diameter of all 34 contralateral invasive carcinomas was significantly smaller (Student's *t*-test; $P < 0.05$; Fig. 3): 14 mm (sd = 7 mm; range 5–33 mm). Fifteen of 40 invasive primary carcinomas (37.5%) presented more than one mass in the ipsilateral breast. Regarding the contralateral breast, only 3 of 34 invasive malignancies (8.8%) revealed

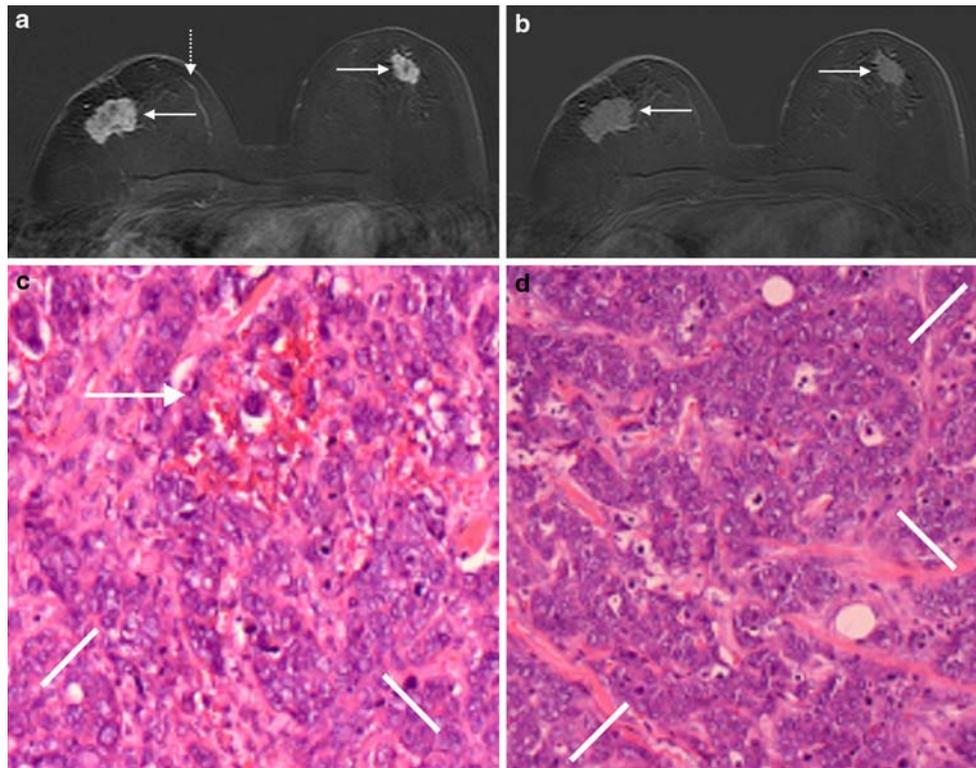


Fig. 2 The MR subtraction images 1 min (a) and 7 min (b) after bolus injection demonstrates a strong initial signal increase with wash-out sign of the bilateral masses (continuous arrows). The shape of both carcinomas is irregular. Both masses are located in the retromamillar part of the breast. The primary index carcinoma on the right side additionally shows prominent vessels (discontinuous

arrow). The histopathologic images (hematoxylin–eosin; original magnification $\times 100$; c, d) reveal characteristics of bilateral low-differentiated invasive ductal carcinomas. The tumor cells (lines) show prominent nuclei and many mitotic figures. The carcinoma on the right (c) additionally demonstrates tumor infiltration of a capillary (arrow)

more than one mass in the same breast (Fisher's exact test; $P < 0.05$).

The tumor infiltration of the pectoralis muscle and the cutis also differed between the primary index versus the contralateral carcinomas. Two of 42 primary index carcinomas (4.8%) showed an infiltration of the pectoralis muscle with pathologic enhancement of the muscle; 11 of 42 primary index carcinomas (26.2%) infiltrated the cutis demonstrating amongst other features skin thickening (Fig. 3). Whereas, none of the contralateral carcinomas presented infiltration of the pectoralis muscle or the cutis. In 7 of 42 primary index cancers (16.7%), the nipple showed pathologic nodular enhancement and an increased thickening at the primary index side indicating a nipple infiltration (Fig. 3). In comparison, only 2 of 42 contralateral carcinomas (4.8%) presented a pathologic nipple. This difference did not reveal statistical significance (Fisher's exact test; $P > 0.05$). The lymph node involvement was significantly different: 12 of 42 primary index carcinomas (28.6%) showed histologically positive ipsilateral axillary lymph node involvement; whereas, the axillary lymph nodes on the same side were only infiltrated in 3 of 42 contralateral invasive carcinomas (7.1%).

Masses and non-mass-like enhancement

All of the invasive breast carcinomas, i.e., 40 primary index carcinomas and 34 contralateral carcinomas, showed masses in MRI. In contrast, the carcinomas in situ, i.e., 2 primary index carcinomas and 8 contralateral ones, were classified as non-mass-like enhancements without existence of a mass. Furthermore, in invasive carcinomas, a non-mass-like enhancement indicating extensive intraductal component (EIC) was detected adjacent to the tumor masses in 14 of 40 primary index carcinomas (35.0%) and in 8 of 34 contralateral carcinomas (23.5%). Thus, regarding invasive and non-invasive carcinomas together, in 16 of 42 primary index (38.1%) and in also 16 of 42 contralateral carcinomas (38.1%), a non-mass-like enhancement was observed, either solely or adjacent to masses. In 30 of 42 bilateral cancer pairs (71.4%), both breasts simultaneously presented a non-mass-like enhancement or did not show any; the correlation coefficient Phi was 0.394 ($P < 0.05$). In detail, 10 of the 42 bilateral carcinomas (23.8%) showed at both sides a non-mass-like enhancement, and 20 of the 42 bilateral cancer pairs (47.6%) did not present any, neither at the primary index nor at the contralateral side.

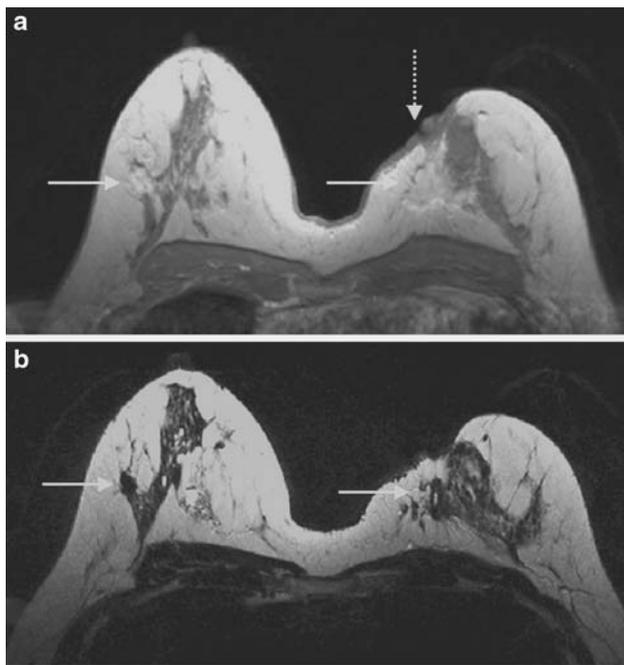


Fig. 3 The T1-weighted sequence 1 min after bolus injection (**a**) and the T2-weighted image (**b**) demonstrates an advanced primary index carcinoma on the left breast and a smaller 8 mm contralateral carcinoma (continuous arrows). Both masses are hypointense in the T2-weighted image. The primary index carcinoma additionally shows an infiltration of the cutis and the nipple (discontinuous arrow)

Dynamic parameters

For masses, the initial signal increase and the postinitial enhancement were similar between the bilateral carcinomas (Table 2). In 75.8% ($n = 25$), the initial signal increase, and in 66.7% ($n = 22$), the postinitial curve types were congruent between the 33 primary index and the 33 corresponding contralateral carcinomas (Table 2; Fig. 2).

Regarding the curve types of the detected non-mass-like enhancements, 9 of 16 primary index carcinomas presented continuous signal increase, 3 of 16 a curve type with plateau phenomenon, and 4 of 16 a wash-out curve. In comparison, 12 of the 16 non-mass-like enhancements of the contralateral carcinomas showed a continuous signal

increase, and 2 of 16 a curve with plateau phenomenon and further 2 of 16 a wash-out sign. Regarding the 10 bilateral carcinomas presenting a non-mass-like enhancement at both tumor sides, half of the enhancements ($n = 5$) had a congruent signal curve type.

Morphology of the masses

Based on the BI-RADS criteria, the shape and the margin of the detected masses were in more than half of the cases similar between the primary index and the corresponding contralateral tumors (Table 3; Fig. 2). The masses bilaterally showed a hyper-, iso-, or hypointense signal intensity in T2-weighted images in 81.8% ($n = 27$) of 33 invasive carcinomas (Fig. 3). Blooming sign was evaluated as a further morphologic parameter, which was defined as the phenomenon that 1 min after bolus injection a fast enhancing lesion presents a sharply configured border; the lesion's rim becomes more and more unsharp up to 7 min after contrast media administration. The blooming sign occurred with approximately the same prevalence in the primary index and the contralateral carcinoma (Fisher's exact test; $P > 0.05$). In 69.7% ($n = 23$) of 33 invasive carcinomas, the blooming phenomenon was synchronously detected in the primary index and the corresponding bilateral cancer or could not be observed in neither of the bilateral masses (Table 3). The parameter adjacent vessel is defined as a prominent enlarged vessel feeding a mass. More primary index invasive carcinomas presented an adjacent vessel in comparison with the contralateral malignant invasive tumors (Fisher's exact test; $P < 0.05$).

Morphology of the non-mass-like enhancements

The majority of the 16 detected non-mass-like enhancements at the primary index breast showed segmental spatial distribution, in detail 9 of 16. The other spatial distributions of the non-mass-like enhancements at the primary index site were: 2 linear/ductal, 3 regional, 1 multiple regions, and 1 diffuse. The following spatial distributions of the 16 non-mass-like enhancements were detected at the

Table 2 Comparison of dynamic parameters of the masses in invasive primary index and invasive contralateral carcinomas

	Primary index carcinomas ($n = 40$)	Contralateral carcinomas ($n = 34$)	Congruence of occurrence in both breasts ($n = 33$)	Correlation coefficient
<i>Initial signal increase</i>				
<100%	10 (25.0)	12 (35.3)	25 (75.8)	Phi = 0.419*
>100%	30 (75.0)	22 (64.7)		
<i>Postinitial enhancement</i>				
Continuous increase	3 (7.5)	3 (8.8)	22 (66.7)	Cramer's V = 0.399*
Plateau phenomenon	9 (22.5)	13 (38.2)		
Wash-out sign	28 (70.0)	18 (52.9)		

Numbers in parentheses are percentages

* $P < 0.05$

Table 3 Comparison of morphologic parameters of the masses in invasive primary index and invasive contralateral carcinomas

	Primary index carcinomas (<i>n</i> = 40)	Contralateral carcinomas (<i>n</i> = 34)	Congruence of occurrence in both breasts (<i>n</i> = 33)	Correlation coefficient
Shape				
Round/oval	13 (32.5)	18 (53.0)		Cramer's <i>V</i> = 0.401*
Lobulated	4 (10.0)	3 (8.8)	17 (51.5)	
Irregular	23 (57.5)	13 (38.2)		
Margin				
Smooth	8 (20.0)	12 (35.3)		Cramer's <i>V</i> = 0.422*
Irregular	20 (50.0)	16 (47.1)	20 (60.6)	
Spiculated	12 (30.0)	6 (17.6)		
Signal intensity in T2-weighted images				
Hypointense	31 (77.5)	23 (67.6)		Cramer's <i>V</i> = 0.770***
Isointense	6 (15.0)	9 (26.5)	27 (81.8)	
Hyperintense	3 (7.5)	2 (5.9)		
Blooming sign	23 (57.5)	17 (50.0)	23 (69.7)	Phi = 0.465**
Adjacent vessel	31 (77.5)	18 (52.9)	20 (60.6)	Phi = 0.238

Numbers in parentheses are percentages

P* < 0.05; *P* < 0.01;

****P* < 0.001

Table 4 Comparison of localization and further morphologic parameters in 42 primary index and contralateral carcinomas

	Primary index carcinomas (<i>n</i> = 42)	Contralateral carcinomas (<i>n</i> = 42)	Congruence of occurrence in both breasts (<i>n</i> = 42)	Correlation coefficient
Main quadrant of the tumor				
Upper outer	21 (50.0)	20 (47.6)		Cramer's <i>V</i> = 0.458**
Upper inner	11 (26.2)	10 (23.8)	26 (61.9)	
Lower outer	6 (14.3)	8 (19.1)		
Lower inner	4 (9.5)	4 (9.5)		
Main localization of the tumor				
Retromamillar	12 (28.6)	13 (30.9)		Cramer's <i>V</i> = 0.484**
Central	23 (54.7)	22 (52.4)	28 (66.7)	
Dorsal	7 (16.7)	7 (16.7)		
Edema	20 (47.6)	9 (21.4)	27 (64.3)	Phi = 0.315
Prominent vessels	26 (61.9)	10 (23.8)	22 (52.4)	Phi = 0.208

Numbers in parentheses are percentages

***P* < 0.01

contralateral side: 8 segmental, 2 linear/ductal, and 6 regional. The internal morphology of the non-mass-like enhancement at the primary index breast was as follows: 6 stippled/punctate, 7 clumped, and 3 dendritic. The 16 non-mass-like enhancements at the contralateral site presented the following internal morphologic patterns: 7 stippled/punctate, 4 clumped, and 5 dendritic. Regarding the 10 bilateral carcinomas presenting a non-mass-like enhancement at both tumor sides, only 4 enhancements bilaterally showed the same spatial distribution pattern, but 8 had a congruent internal morphology.

Localization and morphologic signs of the breast

In 64.3% (*n* = 27) of the 42 evaluated cases, the primary index carcinoma was located in the left breast, in 15 women (35.7%) in the right breast. In the case of that the

carcinomas presented masses, it was determined in which quadrant the majority of the masses were situated. In the absence of masses, the main quadrant was defined where the mostly extended part of the non-mass-like enhancement was detected. The main localization was determined in a similar manner; the breast was divided into three parts: retromamillar, central, and dorsal. In 26 of 42 subjects (61.9%), the main tumor quadrant of the primary index cancer and the corresponding contralateral carcinomas was the same (Table 4). More than half of the primary index carcinomas were mainly located in the central breast region; in the majority of the contralateral carcinomas, the main localization was also central. The main localization of the corresponding bilateral carcinomas was congruent in 28 of 42 cases (66.7%; Fig. 2).

More primary index carcinomas presented edema compared with the contralateral tumors (Fisher's exact test;

$P < 0.05$; Table 4). Twenty of 42 primary index carcinomas (47.6%) showed perifocal edema. In 6 of 42 primary index cancers (14.3%), prepectoral edema was observed; 16.7% ($n = 7$ of 42) revealed edema in a diffuse localization, and in 3 (7.1% of 42) primary index carcinomas, cutaneous/subcutaneous as well as perimamillar edema was detected. No cutaneous/subcutaneous, perimamillar and prepectoral edema was observed in the contralateral site. Eight of 42 contralateral tumors showed perifocal edema; in 4.8% edema was revealed in a diffuse localization. It was furthermore evaluated if the vessels in the breast were prominent in diameter and/or quantity. More primary index carcinomas showed prominent vessels in comparison with the contralateral cancers (Fisher's exact test; $P < 0.01$; Fig. 2). In 52.4% ($n = 22$) of 42 subjects, prominent vessels were simultaneously detected or could not be revealed in both breasts; the Phi correlation analysis did not reach statistical significance (Table 4).

Discussion

Pre-therapeutic cancer staging

Contrast-enhanced MRI has proven benefit in the pre-therapeutic staging of breast carcinomas [9, 10, 16]; it has the potential to lead to a therapeutic change because of the detection of additional cancer foci and a more accurate determination of the tumor extent with an increasing rate of complete tumor excision [13, 16, 33]. According to published results, MRI shows high sensitivity and specificity in the diagnosis of simultaneously developing contralateral carcinomas [13, 21, 34]. In an extended multicenter trial, MRI depicted 3.1% contralateral malignancies in 969 women with a recent diagnosis of unilateral breast cancer [21]. All of these contralateral synchronous carcinomas were missed by X-ray mammography and clinical examination; the sensitivity of MRI in the contralateral breast was 91%, and the specificity was 88% [21].

In our investigation, comparable results were found: MRI was able to detect 2.5% in other breast imaging modalities occult contralateral carcinomas. Compared with the multicenter trial of Lehman et al. [21], we furthermore considered besides X-ray mammographic findings ultrasonographic results. In the study of Fischer et al. [13], contralateral carcinomas not visible by ultrasonography or X-ray mammography were depicted by MRI in 3.2% of the evaluated patients. However, Slanetz et al. [19] reported that MRI identified in 4 of 17 (23.5%) patients a contralateral synchronous cancer occult to physical examination, X-ray mammography, and ultrasonography. Similarly to published reports [13, 21, 34], we included invasive cancers as well as carcinomas in situ. One benefit of our study

design is the standardized MRI protocol and the consistency of histopathologic verifications and clinical data. The focus of our study was set on the comparison of the bilateral carcinomas. To our knowledge, this investigation, which analyzed multiple dynamic and morphologic MRI parameters as well as the histology and the localization of the primary index versus the contralateral cancer, is the first one of its kind.

Histopathologic similarities

The found histologic bilateral similarities are in concordance with the results of Hungness et al. [1], who reported that the histologic types of the bilateral carcinomas were identical in 56.9% of 51 evaluated patients. In the study of Liberman et al. [18], the histologic types of the primary index and the contralateral cancer were the same in 66.7% of 12 women. However, Pediconi et al. [34] published different findings: only 2 of 22 analyzed contralateral malignancies shared the same histologic tumor type as the primary index cancer. However, the initially included patients were significantly younger (mean age = 52 years) than our cohort (mean age = 63 years; Student's *t*-test, $P < 0.05$). In 9 of 22 patients with bilateral carcinomas, DCIS was observed in one site and invasive ductal carcinoma in the other one; one subject showed invasive lobular carcinoma in one and LCIS in the contralateral breast [34]. In situ disease is currently considered as a precursor of invasive breast carcinoma; especially DCIS is likely to progress to invasive ductal carcinoma if left untreated [35]. In our investigation, 4 patients presented DCIS in the contralateral breast and invasive ductal carcinoma in the index one.

There is evidence to suggest that a contralateral breast malignancy is usually a second primary tumor and not a metastatic disease because only a few bilateral carcinomas displays identical of all assessed biologic markers [22, 36]. The presence of an EIC component adjacent to the tumor masses, which could also be detected in many subjects in our investigation, furthermore leads to the conclusion that each of the bilateral carcinomas has generally arisen independently and represents a distinct pathologic entity [6, 22]. There is a controversy if bilateral carcinomas share similar biologic tumor characteristics. Although the biologic phenotypes between contralateral carcinomas are in general not identical, some reports [2, 6] found significant biologic similarities, such as bilateral receptor status. In concordance with our findings, especially the ER status is supposed to display a high bilateral congruence [2, 6]. Kollias et al. [6] proposed that bilateral biologic similarities may result from a common carcinogenic environment, such as hormonal, environmental, or genetic influences; however, alterations may occur during the clonal evolution

of the carcinomas during the tumorigenesis. Biologic similarities, especially hormonal receptor status, can have a significant impact on the treatment concept of bilateral synchronous carcinomas.

Imaging similarities

Possible biologic similarities may be the reason for the detected congruence of many of the evaluated dynamic and morphologic MRI characteristics. Analyzing a few MRI morphologic features, Liberman et al. [18] found the same imaging features of the primary index and the contralateral carcinomas in 66.7% of the subjects. Regarding other breast imaging modalities, imaging congruences between bilateral carcinomas were also reported. Malignant contralateral calcifications were detected more often by X-ray mammography in cases, in whom malignant calcifications were present in the primary index cancer than in those without calcifications in the primary index carcinoma [37].

Comparable with the biologic results, bilateral tumor imaging features are in general similar, but not identical. Combining imaging features, less than half of the lesion pairs show the same bilateral appearance [24, 37, 38]. Of 58 evaluated bilateral carcinomas, Murphy et al. [38] detected in 41.4% on X-ray mammography evident lesion pairs an analogous X-ray mammographic appearance, considering together density, architectural distortion, spiculation, and calcifications. In the study of Lou et al. [24], 18 of 58 bilateral carcinomas (31.0%) presented at least four congruent ultrasonographic characteristics. Regarding the most common ultrasonographic features solely, taller than wide shape ratio, irregular margins and heterogeneous internal echo, the bilateral congruence was 60.3, 70.7, and 74.1%, respectively [24].

The similarities in the dynamic curve types of the bilateral masses may be due to analogous tumor neovascularization, regulated by various cytokines, such as vascular endothelial growth factor [39, 40]. In general, capillaries induced by tumor angiogenesis show a less intact basal membrane; Buadu et al. [40] found that the quantity and distribution of blood microvessels act as a key role in the fast and strong initial signal increase after contrast media administration. The wash-out phenomenon of invasive carcinomas is supposed to be mainly due to arteriovenous anastomoses and the large number of capillaries with a high flow rate, resulting in a rapid transport of contrast media [26, 41]. Morphologic similarities, such as shape and margin of the bilateral masses, may be caused by an analogous tumor infiltration in the surrounding stroma [27, 42]. This mechanism could also explain the congruence of the blooming sign [43]. The highly significant congruence of the T2-signal intensities reflect similarities in the bilateral tumor components, such as desmosplastic or

necrotic reactions [27, 42]. Similarities in imaging appearances of contralateral carcinomas compared with the primary index ones can result in a very intensely specified characterization of frequently detected contralateral lesions in patients with a recent diagnosis of breast cancer [6, 17, 18, 23].

Regarding tumor localizations, a bilateral congruence could also be detected, which may be caused by similarities in the tumorigenesis. Comparable with our results, 31 of 58 (53.4%) X-ray mammographically evident bilateral carcinomas were localized in the same quadrant, published by of Murphy et al. [38]. Previously, contralateral breast biopsies mirroring the location of the primary index cancer had been practiced [44].

Bilateral differences

The evaluated contralateral carcinomas generally had a lower histologic tumor grading and stage than the primary index ones, which is also a consequence of the definition of the bilateral cancers [6, 24, 25]. The fact that the carcinoma of one tumor site is significantly more progressed was described in several investigations [1, 21, 24, 25, 38]. The higher stage of the primary index carcinomas may be the explanation for the higher prevalence of the morphologic parameters edema, adjacent and prominent vessels [27, 30, 45].

The smaller diameter of the contralateral carcinomas is supposed to be one major cause that many of these tumors could not be detected by X-ray mammography and ultrasonography. The histopathology of the 22 occult contralateral malignancies was: 5 carcinomas in situ (3 DCIS, 2 LCIS), 17 invasive cancers (8 lobular, 6 ductal, 2 tubular, and 1 mucinous). In comparison with X-ray mammography and ultrasonography, MRI has to be proven to be valuable in the detection of invasive lobular carcinomas and sub-1 cm malignancies [46, 47]. According to Kuhl et al. [48], MRI has the ability to diagnose by X-ray mammography missed DCIS. In our study, the majority of lesions detected only by MRI occurred predominantly in patients with dense breasts and distinct fibrocystic mathopathy (BI-RADS breast density category III in 10 patients and category IV in 6 patients). The invasive lesions occurring in a non-dense breast, which could only be detected by MRI, were all small ranging from 5 to 7 mm. Equivalent to the investigation of Lehman et al. [21], all of the contralateral cancers, which were only detected by MRM, were lymph node negative in our study.

Limitations

One major limitation of our investigation is the cross-sectional study design at the time of the cancer diagnosis.

Follow-up findings were not evaluated; the prevalence of metachronous bilateral carcinomas and possible false negative MRI findings were therefore not considered. The emphasis of this investigation was to evaluate similarities and differences between the primary index and the corresponding contralateral carcinomas. Because the excellent sensitivity, reaching up to 100%, and high specificity, achieving up to 94%, of diagnosing contralateral invasive and non-invasive carcinomas, has been already evaluated [21, 34], the focus of our investigation was not to reevaluate these data. Due to the intention of a thorough analysis, we included a multitude of different parameters; because of their large quantity we did not combine the different parameters.

Another limitation of our study is that two MRI protocols were used, which share a lot of similarities, but there were some differences, e.g., the field of view and the matrix. Another limitation is that none of the evaluated women were proven to be BRCA-positive or to have another genetically tested predisposition to breast cancer. 23.8% of the women had a positive family history; no significant differences could be revealed for the results between patients with or without positive family history. Because of the lack of genetic tests, it is not possible to compare our findings with studies evaluating hereditary breast carcinomas. Further investigations should analyze more specifically patients with hereditary breast cancer and should integrate an MRI follow-up.

Conclusions

Breast MRI is able to detect contralateral lymph node negative carcinomas, which have been missed by X-ray mammography or ultrasonography. The contralateral carcinomas frequently present similar histologic findings, including tumor type and receptor status, compared with their corresponding primary index cancers. A congruence of bilateral tumor localizations could also be detected. The bilateral malignancies, which are supposed to represent on each site a distinct biologic entity, significantly revealed several similar dynamic and morphologic MRI parameters reflecting analogies of tumor neoangiogenesis, histopathologic components, and infiltration in the surrounding stroma. Phenotypic similarities in bilateral breast cancer should have an impact on a single and therefore cost-effective and for the patient agreeable treatment concept including anti-hormonal and targeted therapy adjuvants.

Acknowledgment This study was independently performed of any type of grants, funds, or industrial support. There is no potential conflict of interest concerning the article.

References

- Hungness ES, Safa M, Shaughnessy EA, Aron BS, Gazder PA, Hawkins HH, Lower EE, Seeskin C, Yassin RS, Hasselgren PO (2000) Bilateral synchronous breast cancer: mode of detection and comparison of histologic features between the two breasts. *Surgery* 128:702–707. doi:10.1067/msy.2000.108780
- Jobsen JJ, van der Palen J, Ong F, Meerwaldt JH (2003) Synchronous, bilateral breast cancer: prognostic value and incidence. *Breast* 12:83–88. doi:10.1016/S0960-9776(02)00278-3
- Heron DE, Komarnicky LT, Hyslop T, Schwartz GF, Mansfield CM (2000) Bilateral breast carcinoma: risk factors and outcomes for patients with synchronous and metachronous disease. *Cancer* 88:2739–2750. doi:10.1002/1097-0142(200006)15:8
- Kollias J, Ellis IO, Elston CW, Blamey RW (2001) Prognostic significance of synchronous and metachronous bilateral breast cancer. *World J Surg* 25:1117–1124
- Chaudary MA, Millis RR, Hoskins EO, Halder M, Bulbrook RD, Cuzick J, Hayward JL (1984) Bilateral primary breast cancer: a prospective study of disease incidence. *Br J Surg* 71:711–714
- Kollias J, Pinder SE, Denley HE, Ellis IO, Wencyk P, Bell JA, Elston CW, Blamey RW (2004) Phenotypic similarities in bilateral breast cancer. *Breast Cancer Res Treat* 85:255–261. doi:10.1023/B:BREA.0000025421.00599.b7
- Poggi MM, Danforth DN, Sciuto LC, Smith SL, Steinberg SM, Liewehr DJ, Menard C, Lippman ME, Lichter AS, Altemus RM (2003) Eighteen-year results in the treatment of early breast carcinoma with mastectomy versus breast conservation therapy: the National Cancer Institute randomized trial. *Cancer* 98:697–702. doi:10.1002/cncr.11580
- Takahashi H, Watanabe K, Takahashi M, Taguchi K, Sasaki F, Todo S (2005) The impact of bilateral breast cancer on the prognosis of breast cancer: a comparative study with unilateral breast cancer. *Breast Cancer* 12:196–202. doi:10.2325/jbcs.12.196
- Kuhl CK (2007) Current status of breast MR imaging. Part 2. Clinical applications. *Radiology* 244:672–691. doi:10.1148/radiol.2443051661
- Orel SG, Schnall MD (2001) MR imaging of the breast for the detection, diagnosis, and staging of breast cancer. *Radiology* 220:13–30
- Kaiser WA, Zeitler E (1989) MR imaging of the breast: fast imaging sequences with and without Gd-DTPA. Preliminary observations. *Radiology* 170:681–686
- Boetes C, Mus RD, Holland R, Barentsz JO, Strijk SP, Wobbes T, Hendriks JH, Ruys SH (1995) Breast tumors: comparative accuracy of MR imaging relative to mammography and US for demonstrating extent. *Radiology* 197:743–747
- Fischer U, Kopka L, Grabbe E (1999) Breast carcinoma: effect of preoperative contrast-enhanced MR imaging on the therapeutic approach. *Radiology* 213:881–888
- Uematsu T, Yuen S, Kasami M, Uchida Y (2009) Comparison of magnetic resonance imaging, multidetector row computed tomography, ultrasonography, and mammography for tumor extension of breast cancer. *Breast Cancer Res Treat* 112:461–474. doi:10.1007/s10549-008-9890-y
- Sardanelli F, Giuseppetti GM, Panizza P, Bazzocchi M, Fausto A, Simonetti G, Lattanzio V, Del Maschio A (2004) Sensitivity of MRI versus mammography for detecting foci of multifocal, multicentric breast cancer in fatty and dense breasts using the whole-breast pathologic examination as a gold standard. *AJR Am J Roentgenol* 183:1149–1157
- Braun M, Pölcher M, Schrading S, Zivanovic O, Kowalski T, Flucke U, Leutner C, Park-Simon TW, Rudlowski C, Kuhn W, Kuhl CK (2009) Influence of preoperative MRI on the surgical

- management of patients with operable breast cancer. *Breast Cancer Res Treat* 111:179–187. doi:[10.1007/s10549-007-9767-5](https://doi.org/10.1007/s10549-007-9767-5)
17. Lee SG, Orel SG, Woo JJ, Cruz-Jove E, Putt ME, Solin LJ, Czerniecki BJ, Schnall MD (2003) MR imaging screening of the contralateral breast in patients with newly diagnosed breast cancer: preliminary results. *Radiology* 226:773–778. doi:[10.1148/radiol.2263020041](https://doi.org/10.1148/radiol.2263020041)
 18. Liberman L, Morris EA, Kim CM, Kaplan JB, Abramson AF, Menell JH, Van Zee KJ, Dershaw DD (2003) MR imaging findings in the contralateral breast of women with recently diagnosed breast cancer. *AJR Am J Roentgenol* 180:333–341
 19. Slanetz PJ, Edmister WB, Yeh ED, Talele AC, Kopans DB (2002) Occult contralateral breast carcinoma incidentally detected by breast magnetic resonance imaging. *Breast J* 8:145–148. doi:[10.1046/j.1524-4741.2002.08304](https://doi.org/10.1046/j.1524-4741.2002.08304)
 20. Rieber A, Merkle E, Böhm W, Brambs HJ, Tomczak R (1997) MRI of histologically confirmed mammary carcinoma: clinical relevance of diagnostic procedures for detection of multifocal or contralateral secondary carcinoma. *J Comput Assist Tomogr* 21:773–779
 21. Lehman CD, Gatsonis C, Kuhl CK, Hendrick RE, Pisano ED, Hanna L, Peacock S, Smazal SF, Maki DD, Julian TB, DePeri ER, Bluemke DA, Schnall MD (2007) MRI evaluation of the contralateral breast in women with recently diagnosed breast cancer. *N Engl J Med* 365:1295–1303
 22. Dawson PJ, Maloney T, Gimotty P, Juneau P, Ownby H, Wolman SR (1991) Bilateral breast cancer: one disease or two? *Breast Cancer Res Treat* 19:233–244
 23. Brennan ME, Houssami N, Lord S, Macaskill P, Irwig L, Dixon JM, Warren RM, Ciatto S (2009) Magnetic resonance imaging screening of the contralateral breast in women with newly diagnosed breast cancer: systematic review and meta-analysis of incremental cancer detection and impact on surgical management. *J Clin Oncol* 27:5640–5649. doi:[10.1200/JCO.2008.21.5756](https://doi.org/10.1200/JCO.2008.21.5756)
 24. Lou L, Cong XL, Yu GF, Li JC, Ma YX (2007) US findings of bilateral primary breast cancer: retrospective study. *Eur J Radiol* 61:154–157. doi:[10.1016/j.ejrad.2006.08.022](https://doi.org/10.1016/j.ejrad.2006.08.022)
 25. Kim MJ, Kim EK, Kwak JY, Park BW, Kim SI, Oh KK (2008) Bilateral synchronous breast cancer in an Asian population: mammographic and sonographic characteristics, detection methods, and staging. *AJR Am J Roentgenol* 190:208–213. doi:[10.2214/AJR.07.2714](https://doi.org/10.2214/AJR.07.2714)
 26. Kuhl CK, Mielcareck P, Klaschik S, Leutner C, Wardelmann E, Gieseke J, Schild HH (1999) Dynamic breast MR imaging: are signal intensity time course data useful for differential diagnosis of enhancing lesions? *Radiology* 211:101–110
 27. Malich A, Fischer DR, Wurdinger S, Böttcher J, Marx C, Facius M, Kaiser WA (2005) Potential MRI interpretation model: differentiation of benign from malignant breast masses. *AJR Am J Roentgenol* 185:964–970. doi:[10.2214/AJR.04.1073](https://doi.org/10.2214/AJR.04.1073)
 28. Baum F, Fischer U, Vosschenrich R, Grabbe E (2002) Classification of hypervascularized lesions in CE MR imaging of the breast. *Eur Radiol* 12:1087–1092. doi:[10.1007/s00330-001-1213-1](https://doi.org/10.1007/s00330-001-1213-1)
 29. American College of Radiology (2003) Breast imaging reporting and data system (BI-RADS) atlas, 4th edn. American College of Radiology, Reston, VA
 30. Kaiser WA (2007) Signs in MR-mammography. Springer, Berlin, Heidelberg, New York
 31. Renz DM, Baltzer PAT, Böttcher J, Thaher F, Gajda M, Camara O, Runnebaum IB, Kaiser WA (2008) Magnetic resonance imaging of inflammatory breast carcinoma and acute mastitis. A comparative study. *Eur Radiol* 18:2370–2380. doi:[10.1007/s00330-008-1029-3](https://doi.org/10.1007/s00330-008-1029-3)
 32. Elston CW, Ellis IO (1991) Pathological prognostic factors in breast cancer. I. The value of histological grade in breast cancer: experience from a large study with long-term follow-up. *Histopathology* 19:403–410
 33. Pengel KE, Loo CE, Teertstra HJ, Muller SH, Wesseling J, Peterse JL, Bartelink H, Rutgers EJ, Gilhuijs KG (2009) The impact of preoperative MRI on breast-conserving surgery of invasive cancer: a comparative cohort study. *Breast Cancer Res Treat* 116:161–169. doi:[10.1007/s10549-008-0182-3](https://doi.org/10.1007/s10549-008-0182-3)
 34. Pediconi F, Catalano C, Roselli A, Padula S, Altomari F, Moriconi E, Pronio AM, Kirchin MA, Passariello R (2007) Contrast-enhanced MR mammography for evaluation of the contralateral breast in patients with diagnosed unilateral breast cancer or high-risk lesions. *Radiology* 243:670–680. doi:[10.1148/radiol.2433060838](https://doi.org/10.1148/radiol.2433060838)
 35. Collins LC, Tamimi RM, Baer HJ, Connolly JL, Colditz GA, Schnitt SJ (2005) Outcome of patients with ductal carcinoma in situ untreated after diagnostic biopsy: results from the Nurses' Health Study. *Cancer* 103:1778–1784. doi:[10.1002/ncr.20979](https://doi.org/10.1002/ncr.20979)
 36. Sterns EE, Fletcher WA (1991) Bilateral cancer of the breast: a review of clinical, histologic, and immunohistologic characteristics. *Surgery* 110:617–622
 37. Roubidoux MA, Lai NE, Paramagul C, Joynt LK, Helvie MA (1996) Mammographic appearance of cancer in the opposite breast: comparison with the first cancer. *AJR Am J Roentgenol* 166:29–31
 38. Murphy TJ, Conant EF, Hanau CA, Ehrlich SM, Feig SA (1995) Bilateral breast carcinoma: mammographic and histologic correlation. *Radiology* 195:617–621
 39. Degani H, Chetrit-Dadiani M, Bogin L, Furman-Haran E (2003) Magnetic resonance imaging of tumor vasculature. *Thromb Haemost* 89:25–33
 40. Buadu LD, Murakami J, Murayama S, Hashiguchi N, Sakai S, Masuda K, Toyoshima S, Kuroki S, Ohno S (1996) Breast lesions: correlation of contrast medium enhancement patterns on MR images with histopathologic findings and tumor angiogenesis. *Radiology* 200:639–649
 41. Sherif H, Mahfouz AE, Oellinger H, Hadijuana J, Blohmer JU, Taupitz M, Felix R, Hamm B (1997) Peripheral washout sign on contrast-enhanced MR images of the breast. *Radiology* 205:209–213
 42. Tse GM, Chaiwun B, Wong KT, Yeung DK, Pang AL, Tang AP, Cheung HS (2007) Magnetic resonance imaging of breast lesions—a pathologic correlation. *Breast Cancer Res Treat* 103:1–10. doi:[10.1007/s10549-006-9352-3](https://doi.org/10.1007/s10549-006-9352-3)
 43. Fischer DR, Baltzer P, Malich A, Wurdinger S, Freesmeyer MG, Marx C, Kaiser WA (2004) Is the “blooming sign” a promising additional tool to determine malignancy in MR mammography? *Eur Radiol* 14:394–401. doi:[10.1007/s00330-003-2055-9](https://doi.org/10.1007/s00330-003-2055-9)
 44. Dawson LA, Chow E, Goss PE (1998) Evolving perspectives in contralateral breast cancer. *Eur J Cancer* 34:2000–2009
 45. Siewert C, Oellinger H, Sherif HK, Blohmer JU, Hadijuana J, Felix R (1997) Is there a correlation in breast carcinomas between tumor size and number of tumor vessels detected by gadolinium-enhanced magnetic resonance mammography? *MAGMA* 5:29–31
 46. Mann RM, Hoogeveen YL, Blickman JG, Boetes C (2008) MRI compared to conventional diagnostic work-up in the detection and evaluation of invasive lobular carcinoma of the breast: a review of existing literature. *Breast Cancer Res Treat* 107:1–14. doi:[10.1007/s10549-007-9528-5](https://doi.org/10.1007/s10549-007-9528-5)
 47. Gibbs P, Liney GP, Lowry M, Kneeshaw PJ, Turnbull LW (2004) Differentiation of benign and malignant sub-1 cm breast lesions using dynamic contrast enhanced MRI. *Breast* 13:115–121. doi:[10.1016/j.breast.2003.10.002](https://doi.org/10.1016/j.breast.2003.10.002)
 48. Kuhl CK, Schrading S, Bieling HB, Wardelmann E, Leutner CC, Koenig R, Kuhn W, Schild HH (2007) MRI for diagnosis of pure ductal carcinoma in situ: a prospective observational study. *Lancet* 370:485–492. doi:[10.1016/S0140-6736\(07\)61232-X](https://doi.org/10.1016/S0140-6736(07)61232-X)